

Ultrafast X-ray spectroscopy of conical intersections

Simon P. Neville^{1,2}, Majed Chergui², Albert Stolow^{1,3,4}, and Michael S. Schuurman^{1,3}

¹*Department of Chemistry and Biomolecular Sciences, University of Ottawa,
10 Marie Curie, Ottawa, Ontario, K1N 6N5, Canada*

²*Ecole Polytechnique Fédérale de Lausanne, Laboratoire de Spectroscopie
Ultrarapide and Lausanne Centre for Ultrafast Science (LACUS),
Faculté des Sciences de Base, ISIC, Lausanne CH-1015, Switzerland*

³*National Research Council of Canada, 100 Sussex Drive, Ottawa, Ontario K1A 0R6, Canada and*

⁴*Department of Physics, University of Ottawa, 150 Louis Pasteur, Ottawa, ON K1N 6N5 Canada*

Ongoing developments in ultrafast X-ray sources offer powerful new means of probing the complex non-adiabatically coupled structural and electronic dynamics of photoexcited molecules. These non-Born-Oppenheimer effects are governed by general electronic degeneracies termed conical intersections which play a key role, analogous to that of a transition state, in the electronic-nuclear dynamics of excited molecules. Using high level *ab initio* quantum dynamics simulations, we studied time-resolved X-ray absorption and photoelectron spectroscopy (TRXAS and TRXPS, respectively) of the prototypical unsaturated organic chromophore, ethylene, following excitation to its $S_2(\pi\pi^*)$ state. The TRXAS in particular is highly sensitive to all aspects of the ensuing dynamics. These X-ray spectroscopies provide a clear signature of the wavepacket dynamics near conical intersections, related to charge localization effects driven by the nuclear dynamics. Given the ubiquity of charge localization in excited state dynamics, we believe that ultrafast X-ray spectroscopies offer a unique and powerful route to the direct observation of dynamics around conical intersections.

In excited states of polyatomic molecules, conical intersections (CIs) play a central role, analogous to transition states in ground state dynamics. The spatial range of the conical intersection dynamics is somewhat extended beyond the CI (a point of electronic degeneracy) itself. In the following, we use the general term conical intersection to refer to this spatial region. Despite their widespread use in rationalizing ultrafast electronic-nuclear dynamics[1], unambiguous experimental observation of CIs remains elusive. Here we investigate the use of ultrafast X-ray spectroscopies to directly observe dynamics at CIs. This is motivated by recent technological advances which result in the availability of powerful ultrafast light sources in the X-ray regime. The use of X-rays is appealing because they offer an atom-specific probe of electronic and structural dynamics. While most X-ray spectroscopic studies of molecular dynamics were initially performed in the hard X-ray range[2–4], studies have also recently appeared in the soft X-ray range[5], in particular using table-top sources[6, 7].

There is a growing number of theoretical proposals for the use of X-ray spectroscopies to probe the ultrafast nonadiabatic dynamics in photoexcited molecules[8–13]. Of these, only two techniques, namely Time-Resolved X-ray Absorption Spectroscopy (TRXAS) and Time-Resolved X-ray Photoelectron Spectroscopy (TRXPS), have demonstrated experimental feasibility and are therefore the focus of the present study. We recently showed that the pre-edge region of the X-ray absorption spectrum offers a uniquely sensitive probe of dynamics in the most fundamental unsaturated hydrocarbon, the planar C_2H_4 molecule ethylene[9]. Specifically, the computed time-resolved Carbon K-edge absorption spectrum contained clear signatures of the excited state

wavepacket dynamics[9, 10]. Here we apply this approach to the spectroscopy of conical intersections, an important goal of ultrafast molecular sciences. In our previous work on valence shell time-resolved photoelectron spectroscopy (TRPES), we showed that the outgoing photoelectron is a particularly insightful probe of nonadiabatic dynamics in molecules[14–16]. Therefore, we also simulate here the inner shell time-resolved X-ray photoelectron spectrum (TRXPS) for the same photo-initiated process. We believe that this comparison will help design the next generation of X-ray spectroscopy experiments which are just emerging[6, 7, 17].

Via our simulations, we have uncovered a key advantage of ultrafast X-ray spectroscopy: that charge localization effects in photo-excited ethylene lead to large (few eV) splittings in the excited state pre-edge X-ray absorption spectrum. This, in turn, offers a unique and acute sensitivity to wavepacket dynamics at a CI. This observation has far reaching consequences, given the commonality of charge localization in excited state molecular dynamics and biological processes such as proton and electron transfer.

Our methods for calculating TRXAS were described in detail elsewhere[9]. Likewise, our simulations of TRXPS are directly analogous to previously described methodologies for computing valence shell electron (UV) TRPES[18]. Accordingly, we give only a brief summary of the computational methodology here, with further details offered in the Supplemental Information. The *ab initio* multiple spawning (AIMS) method[19] was used to describe the time evolution of the excited state wavepacket. In the AIMS method, the molecular wavefunction is expanded in a set of adiabatic electronic functions, $\{|I(\mathbf{r}; \mathbf{R})\rangle\}$, and frozen Gaussian nuclear basis

functions, $\{|g_j^{(I)}(\mathbf{R}, t)\rangle\}$, of the Heller form:

$$|\Psi(\mathbf{R}, \mathbf{r}, t)\rangle = \sum_{I=1}^{n_s} \sum_{j=1}^{N_I} C_j^{(I)}(t) |g_j^{(I)}(\mathbf{R}, t)\rangle |I(\mathbf{r}; \mathbf{R})\rangle. \quad (1)$$

The positions and momenta of the Gaussian basis functions evolve according to the classical equations of motion, and the expansion coefficients are evolved variationally via the solution of the time-dependent nuclear Schrödinger equation. The AIMS equations of motion were solved on-the-fly using the results of electronic structure calculations performed at the multireference first order configuration interaction (MR-FOCI) level of theory. The details of these calculations are given in the Supplementary Information.

In Figure 1 we schematically shows the relevant electronic states as a function of the torsional angle between the two planes defined by each of the CH_2 groups in the molecule. Following vertical excitation of the $S_2(\pi\pi^*)$ state, the wavepacket is localized at the structural and electronic character labeled “A”. In line with previous studies[20–23], a rapid evolution of the initially excited S_2 state occurs by large amplitude twisting motion about the C-C bond, leading to a change in electronic character. The S_1 state is transiently populated and has an electronic structure characterized by both valence $\pi\pi^*$ and Rydberg $\pi 3s$ character (point “B”). The total excited state lifetime was determined to be ~ 95 fs. Internal conversion to the S_0 ground state is found to occur via so-called twisted-pyramidalized (Tw-Py) CI seam (point “CI”). This CI structure involves a 90° twist about the C-C double bond combined with pyramidalization at one of the C atoms.

We first examine the ability of TRXAS to probe this coupled electronic and nuclear dynamics. The pre-edge part of the TRXAS, $\sigma(E, t)$, was calculated as an incoherent sum over the transient spectra at the centres of the Gaussian basis functions:

$$\sigma(E, t) = \sum_{I=1}^{n_s} \sum_{j=1}^{N_I} |C_j^{(I)}(t)|^2 \sigma_I(E; \bar{\mathbf{R}}_j^{(I)}(t)). \quad (2)$$

Here, $\sigma_I(E; \bar{\mathbf{R}}_j^{(I)}(t))$ denotes the X-ray absorption spectrum (XAS) for the I th electronic state calculated at the centre $\bar{\mathbf{R}}_j^{(I)}(t)$ of the Gaussian basis function $g_j^{(I)}(t)$. The XAS were calculated using the second-order algebraic diagrammatic construction method within the core-valence separation approximation[24] (CVS-ADC(2)) and the 6-311++G** basis.

In Figure 2 (a) we show the time evolution of the C K-edge XANES spectrum following excitation to the $S_2(\pi\pi^*)$ state, while Figure 2 (b) focuses on the pre-edge region only (< 295 eV). The post-edge NEXAFS region

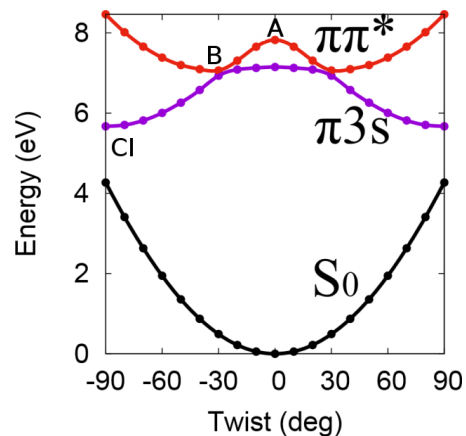


FIG. 1. Relevant electronic states in ethylene as a function of the torsional angle about the C-C bond. The dynamics simulation initializes the wave packet at the FC geometry on the $S_2(\pi\pi^*)$ state (point “A”). The crossing between the initial $\pi\pi^*$ state and the $\pi 3s$ state is denoted “B”. The important conical intersection with the ground state is labeled “CI” and is the dynamical gateway (“transition state”) for the excited state.

reflects structural dynamics in the excited molecule and will be discussed in a future publication. Feature “A” at $t=0$ and 277 eV is assigned to excitation of initially prepared $\pi\pi^*$ state to the $1s\pi^*$ core-excited state[9]. The sweep of this feature to higher energies is a result of rapid twisting about the C-C bond, lowering the energy of the $\pi\pi^*$ state. Feature “B”, beginning at around 281 eV and 10 fs, corresponds to two components of the wavepacket: (i) the portion in the transiently populated $\pi 3s$ state which transitions to the $1s3s$; (ii) the component passing through the Tw-Py CI seam. The feature labeled “CI”, centred around 286 eV begins to develop intensity at around ~ 10 fs. It is also assigned to core-excitation from the $\pi\pi^*$ state. Significantly, the “CI” feature originates only from those components of the wavepacket in the $\pi\pi^*$ state that are in close proximity to the Tw-Py CI seam. In other words, the calculated TRXAS reveals a clear and direct signature of the arrival of the excited state wavepacket at the CI. Finally, the broad, intense set of peaks appearing at times $t \gtrsim 50$ fs in Figure 2 (a) corresponds to the vibrationally hot ground electronic state which appears following passage through the CI.

The most remarkable feature of the calculated TRXAS is that it clearly encodes the arrival of the wavepacket at the Tw-Py CI. Figures S1-S5 in the supplemental material[25] show the XAS calculated at two relevant geometries for the states involved and is a convenient reference for the following discussion. Importantly, we find that at geometries close to the Tw-Py CI geometry, a remarkable splitting appears in the higher energy peak for the $\pi\pi^*$ state (corresponding to the S_1 state at this geometry) pre-edge XAS. At the initial Franck-

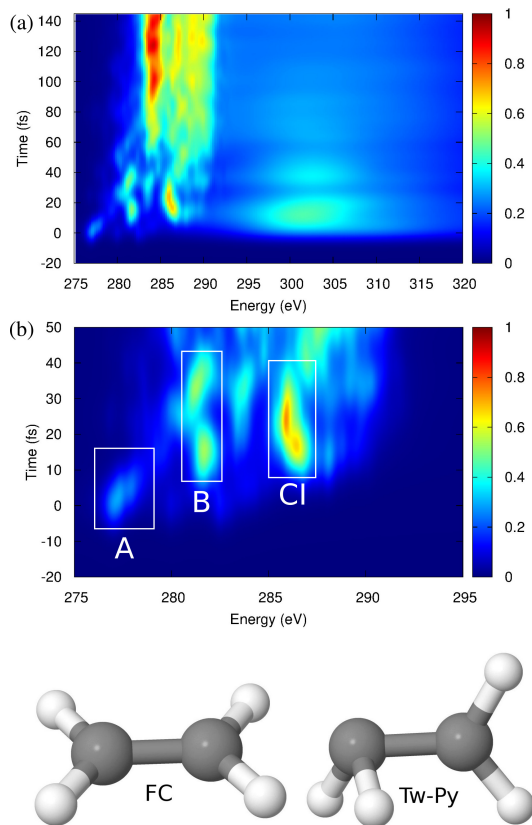


FIG. 2. The TRXAS spectrum calculated from AIMS simulations of ethylene excited to its $\pi\pi^*$ state. (a) The full spectrum showing both the pre-edge and post-edge continuum absorption. (b) The pre-edge part of the spectrum at short times and the relevant peak assignments. The features labeled “A”, “B” and “CI” are directly related to the associated dynamical features shown in Figure 1. The FC (“A”) and Tw-Py intersection (“CI”) geometries are shown below. The color map represents the relative probability of absorption.

Condon (FC), point labeled “A”, the $\pi\pi^*$ state pre-edge XAS is dominated by a single transition corresponding to the excitation of a $1s$ core electron into the hole in the singly-occupied π orbital. At the FC point, the molecule possesses D_{2h} symmetry, meaning that the two $1s$ orbitals are delocalized across the two indistinguishable C atoms, and only excitation from the a_g $1s$ orbital into the π orbital is dipole allowed. That is, only one $1s \rightarrow \pi$ transition is dipole allowed at this point. Upon pyramidalization at one of the C atoms, the symmetry is lowered and the two C atoms now become distinguishable. The consequences of this are twofold: (i) the $1s$ orbitals now become localized about the C atoms; (ii) excitation from both of these $1s$ orbitals into the π orbital hole now becomes dipole allowed. Accordingly, two $1s \rightarrow \pi$ transitions now appear in the XAS. Importantly, as we discuss below, the splitting between the two transition energies is quite large, ~ 4.5 eV, due to the significant

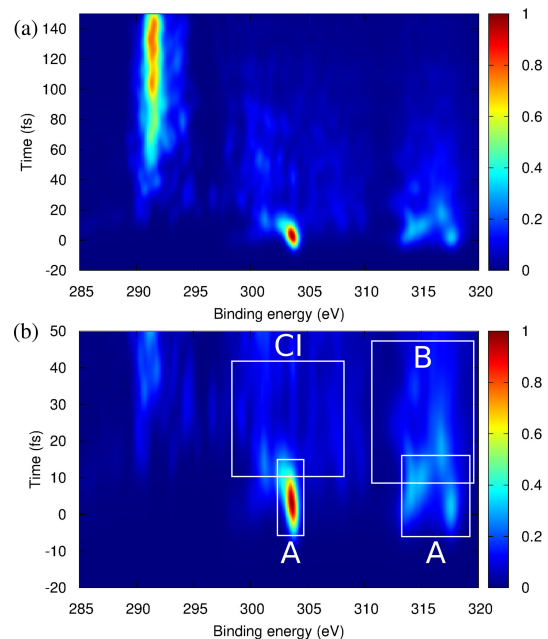


FIG. 3. TRXPS calculated using the results of AIMS simulations of ethylene excited to the $\pi\pi^*$ state. A probe photon energy of 320 eV is assumed. (a) The spectrum for all simulation times. (b) The spectrum focused on short times. The features labeled “A”, “B” and “CI” are related to the dynamical features shown in Figure 1. The color map represents the relative probability of ionization.

difference in the local valence electronic structure that develops around the two C atoms. In other words, the charge separation driven by the non-adiabatic dynamics is probed in an atom-specific manner by absorption from each of the now localised, distinguishable $1s$ orbitals.

Since the nonadiabatic AIMS dynamics simulations which underlie the TRXAS spectrum are identical to those used in the calculated TRXPS spectrum, the relative sensitivities of these two techniques to dynamics at CIs can be compared. In Figure 3 we show the AIMS simulation of the TRXPS spectrum for these same molecular dynamics. At time $t = 0$, the TRXPS is dominated by a single peak corresponding to ionization of the initially prepared $\pi\pi^*$ state in the FC region. Interestingly, the fingerprints of the dynamical evolution are somewhat less clear than in the TRXAS.

Figures S6-S10 show the static X-ray photoelectron spectra (320 eV) at two key geometries (FC “A” and Tw-Py “CI”) for ionization from the relevant electronic states. At early time delays, feature “B” in the 314-318 eV region in Figure 3 shows ionization from $\pi 3s$, but is overlapped with allowed ionization channels from the $\pi\pi^*$ FC geometry “A”, as well ionization from S_1 at the Tw-Py CI. Regarding the latter, the splitting of the two inequivalent C $1s$ centres at the Tw-Py CI manifests itself in the splitting between the group of two peaks centred

at 299 eV and the group of two peaks at 306 eV in Figure S9. However, in the wave packet simulation, these peaks overlap somewhat with the bright peak near 304 eV corresponding to ionization of the initially prepared $\pi\pi^*$, obscuring somewhat the signature of the CI.

Confirmation of the origin of this large splitting of the core excitation energies close to the Tw-Py CI comes from consideration of a one-particle, one-hole (1p1h) excitation operator $\hat{C}_{\nu c} = \hat{c}_\nu^\dagger \hat{c}_c$ applied to the correlated ground electronic state $|\Psi_0\rangle$ to yield the singly core-excited configuration $|\Psi_{\nu c}\rangle = \hat{C}_{\nu c}|\Psi_0\rangle$, where c indexes a core orbital and ν a virtual valence orbital. Applying second-order perturbation theory, the core-excitation energy $\Delta E_{\nu c}$ obtained using the unperturbed 1p1h configuration $|\Psi_{\nu c}\rangle$ can be written as[26, 27]:

$$\Delta E_{\nu c} = [\epsilon_\nu - \epsilon_c] + [2\langle c\nu|\nu c\rangle - \langle c\nu|c\nu\rangle] + \Delta E_{\nu c}^{(2)}. \quad (3)$$

Here, ϵ_p denotes the energy of the p th canonical Hartree-Fock orbital. At the Tw-Py CI geometry, the splitting of the two pre-edge $\pi\pi^*$ state peaks is accounted for almost entirely by the zeroth-order term $[\epsilon_\nu - \epsilon_c]$. Importantly, the splitting of the two peaks is a consequence of the splitting of the corresponding $1s$ orbital energies due to the distinguishability of the two C atoms which occurs uniquely at the CI.

The physical picture emerging from this analysis is that the splitting of the C $1s$ peaks is correlated with the onset of charge separation across the C-C bond (the so-called sudden polarization effect)[28] which occurs uniquely at the CI. To show this, we use the following metric for charge separation, $\Theta(t)$, across the C-C bond derived from the AIMS simulation:

$$\Theta(t) = \sum_{I=1}^{n_s} \sum_{j=1}^{N_I} \left| C_j^{(I)}(t) \right|^2 \left| \left\langle g_j^{(I)}(t) \left| \langle I | \boldsymbol{\mu} \cdot \boldsymbol{\nu}_{CC} | I \rangle \right| g_j^{(I)}(t) \right\rangle \right|. \quad (4)$$

Here, $\boldsymbol{\mu}$ denotes the molecular dipole operator, and $\boldsymbol{\nu}_{CC}$ the unit vector coincident with the C-C bond. The nuclear part of the integral $\langle g_j^{(I)}(t) | \langle I | \boldsymbol{\mu} \cdot \boldsymbol{\nu}_{CC} | I \rangle | g_j^{(I)}(t) \rangle$ is evaluated analytically, whilst the electronic part is evaluated using a first-order saddle point approximation. The short-time evolution of $\Theta(t)$ is shown in Figure 4. It is clear that charge separation across the C-C bond occurs rapidly, with a local maximum value of Θ being attained at around 10 fs. This correlates with the appearance and initial growth in intensity of the peak centred at 286 eV in the calculated TRXAS (Figure 2). The onset of charge separation at the CI leads to the splitting of the peaks in $\pi\pi^*$ state pre-edge XAS. The magnitude of this splitting is a consequence of the separation of the $1s$ orbital energies, as a result of the transient charge separation across the C-C bond that occurs uniquely at the CI. We expect this to be a general feature of dynamics at CIs in

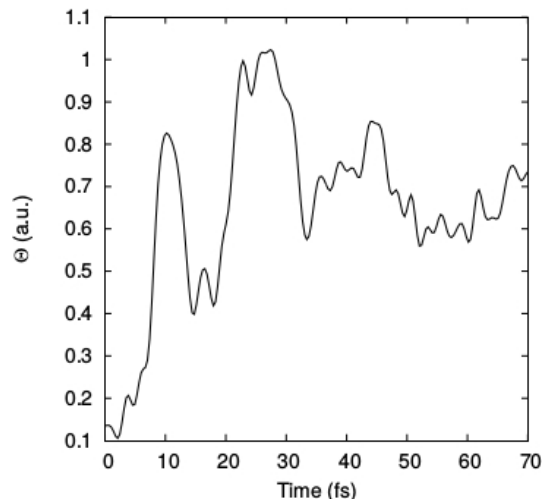


FIG. 4. Time-evolution of the charge transfer metric Θ calculated using the results of AIMS simulations of ethylene excited to the $\pi\pi^*$ state. The large, transient charge separations occur when the wavepacket encounters the Tw-Py CI and is responsible for the distinguishability of the two C atoms at the CI.

molecules containing C=C double bonds. Such molecules play central roles in photochemistry, photobiology and material science.

On the basis of these AIMS simulations, we are emboldened to draw some conclusions. Firstly, employing core electrons to probe valence electron density via ultrafast X-ray spectroscopy results in an exquisitely sensitive measure of complex, dynamic electronic structures. While both TRXAS and TRXPS encode the nonadiabatic dynamics, the overlapping continua in the TRXPS may tend to obscure the CI dynamics. In contrast, TRXAS has fewer dipole-allowed transitions, leading to a direct mapping of absorption peaks to specific dynamical features. We conclude that ultrafast X-ray spectroscopy is a particularly powerful probe of dynamics at conical intersections. The commonality of charge separation dynamics (e.g. proton or electron transfer) in molecular and material processes suggests that TRXAS and TRXPS will have broad applicability, leading to a ‘transition state spectroscopy’ for the excited state. Work is now in progress, within our group and elsewhere, to implement these findings experimentally.

Acknowledgements: M.S. and A.S. acknowledge the support of the National Science and Energy Research Council (Canada) via the Discovery Grants program. MC acknowledges support of the NCCR:MUST of the Swiss NSF.

-
- [1] W. Domcke, D. R. Yarkony, and H. Köppel, “Conical intersections: Electronic structure, dynamics and spectroscopy,” (World Scientific Publishing, 2004) Chap. 1, p. 3.
- [2] C. Bressler, C. Milne, V.-T. Pham, A. ElNanhhas, R. M. van der Veen, W. Gawelda, S. Johnson, P. Beaud, D. Grolimund, M. Kaiser, C. N. Borca, G. Ingold, R. Abela, and M. Chergui, *Science* **323**, 489 (2009).
- [3] H. T. Lemke, C. Bressler, L. X. Chen, D. M. Fritz, K. J. Gaffney, A. Galler, W. Gawelda, K. Haldrup, R. W. Hartsock, H. Ihee, J. Kim, K. H. Kim, J. H. Lee, M. M. Nielsen, A. B. Stickerath, W. Zhang, D. Zhu, and M. Cammarata, *The Journal of Physical Chemistry A* **117**, 735 (2013).
- [4] W. Zhang, R. Alonso-Mori, U. Bergmann, C. Bressler, M. Chollet, A. Galler, W. Gawelda, R. G. Hadt, R. W. Hartsock, T. Kroll, K. S. Kjær, K. Kubicek, H. T. Lemke, H. W. Liang, D. A. Meyer, M. M. Nielsen, C. Purser, J. S. Robinson, E. I. Solomon, Z. Sun, D. Sokaras, T. B. van Driel, G. Vankó, T.-C. Weng, D. Zhu, and K. J. Gaffney, *Nature* **509**, 345 EP (2014).
- [5] N. Huse, H. Cho, K. Hong, L. Jamula, F. M. F. de Groot, T. K. Kim, J. K. McCusker, and R. W. Schoenlein, *The Journal of Physical Chemistry Letters* **2**, 880 (2011).
- [6] A. R. Attar, A. Bhattacharjee, C. D. Pemmaraju, K. Schnorr, K. D. Closser, D. Prendergast, and S. R. Leone, *Science* **356**, 54 (2017).
- [7] Y. Pertot, C. Schmidt, M. Matthews, A. Chauvet, M. Huppert, V. Svoboda, A. von Conta, A. Tehlar, D. Baykusheva, J.-P. Wolf, and H. J. Wörner, *Science* (2017).
- [8] G. Capano, C. J. Milne, M. Chergui, U. Rothlisberger, I. Tavernelli, and T. J. Penfold, *Journal of Physics B: Atomic, Molecular and Optical Physics* **48**, 214001 (2015).
- [9] S. P. Neville, V. Averbukh, S. Patchkovskii, M. Ruberti, R. Yun, M. Chergui, A. Stolow, and M. S. Schuurman, *Faraday Discuss.* **194**, 117 (2016).
- [10] S. P. Neville, V. Averbukh, M. Ruberti, R. Yun, S. Patchkovskii, M. Chergui, A. Stolow, and M. S. Schuurman, *J. Chem. Phys.* **145**, 144307 (2016).
- [11] M. Kowalewski, K. Bennett, K. E. Dorfman, and S. Mukamel, *Phys. Rev. Lett.* **115**, 193003 (2015).
- [12] W. Hua, S. Oesterling, J. D. Briggs, Y. Zhang, H. Ando, R. de Vivie-Riedle, B. P. Fingerhut, and S. Mukamel, *Struct. Dyn.* **3**, 023601 (2016).
- [13] M. Kowalewski, B. P. Fingerhut, K. E. Dorfman, K. Bennett, and S. Mukamel, *Chem. Rev.* **117**, 12165 (2017).
- [14] A. Stolow, A. E. Bragg, and D. M. Neumark, *Chem. Rev.* **104**, 1719 (2004).
- [15] O. Schalk, A. E. Boguslavskiy, A. Stolow, and M. S. Schuurman, *J. Am. Chem. Soc.* **133**, 16451 (2011).
- [16] S. P. Neville, Y. Wang, A. E. Boguslavskiy, A. Stolow, and M. S. Schuurman, *The Journal of Chemical Physics* **144**, 014305 (2016).
- [17] A. Johnson, L. Miseikis, D. Wood, D. Austin, C. Brahm, S. Jarosch, C. Strueber, P. Ye, and J. Marangos, *Structural Dynamics* **3**, 062603 (2016).
- [18] H. R. Hudock, B. G. Levine, A. L. Thompson, H. Satzger, D. Townsend, N. Gador, S. Ullrich, A. Stolow, and T. J. Martínez, *J. Phys. Chem. A* **111**, 8500 (2007).
- [19] M. Ben-Nun and T. J. Martínez, *Adv. Chem. Phys.* **121**, 439 (2002).
- [20] T. Mori, W. J. Glover, M. S. Schuurman, and T. J. Martínez, *J. Phys. Chem. A* **116**, 2808 (2012).
- [21] E. G. Champenois, N. H. Shivaram, T. W. Wright, C. S. Yang, A. Belkacem, and J. P. Cryan, *J. Chem. Phys.* **144**, 014303 (2016).
- [22] T. Kobayashi, T. Horio, and T. Suzuki, *J. Phys. Chem A* **119**, 9518 (2015).
- [23] T. K. Allison, H. Tao, W. J. Glover, T. W. Wright, A. M. Stooke, C. Khurmi, J. van Tilborg, Y. Liu, R. W. Falcone, T. J. Martínez, and A. Belkacem, *J. Chem. Phys.* **136**, 124317 (2012).
- [24] J. Wenzel, A. Holzer, M. Wormit, and A. Dreuw, *J. Chem. Phys.* **142**, 214104 (2015).
- [25] See Supplemental Material at [insert URL] for details on the wave packet simulations, as well as additional X-ray absorption and photoelectron spectra employed for interpretation of the time-resolved data. This material includes references [29-35].
- [26] J. Schirmer, *Phys. Rev. A* **26**, 2395 (1982).
- [27] J. Schirmer, M. Braunstein, M. T. Lee, and V. McKoy, “Vuv and soft x-ray photoionization,” (Plenum Press, New York, 1996) Chap. 4, p. 105.
- [28] B. R. Brooks and H. F. Schaefer, *J. Am. Chem. Soc.* **101**, 307 (1979).
- [29] B. T. Pickup, *Chem. Phys.* **19**, 193 (1977).
- [30] M. Spanner, S. Patchkovskii, C. Zhou, S. Matsika, M. Kottur, and T. C. Weinacht, *Phys. Rev. A* **86**, 053406 (2012).
- [31] B. O. Roos, M. P. Fülcher, P. A. Malmqvist, M. Merchán, and L. Serrano-Andrés, “Quantum mechanical electronic structure calculations with chemical accuracy,” (Kluwer Academic Dordrecht, The Netherlands, 1995) p. 357.
- [32] H. Lischka, R. Shepard, I. Shavitt, R. M. Pitzer, M. Dallos, T. Mller, P. G. Szalay, F. B. Brown, R. Ahlrichs, H. J. Bhm, A. Chang, D. C. Comeau, R. Gdanitz, H. Dachsel, C. Ehrhardt, M. Ernzerhof, P. Hchtl, S. Irle, G. Kedziora, T. Kovar, V. Parasuk, M. J. M. Pepper, P. Scharf, H. Schiffer, M. Schindler, M. Schler, M. Seth, E. A. Stahlberg, J.-G. Zhao, S. Yabushita, Z. Zhang, M. Barbatti, S. Matsika, M. S. Schuurman, D. R. Yarkony, S. R. Brozell, E. V. Beck, , J.-P. Blaudeau, M. Ruckebauer, B. Sellner, F. Plasser, and J. J. Szymczak, “Columbus, an ab initio electronic structure program, release 7.0,” (2012).
- [33] J. F. Stanton, J. Gauss, M. E. Harding, P. G. Szalay, A. A. Auer, R. J. Bartlett, U. Benedikt, C. Berger, D. E. Bernholdt, Y. J. Bomble, L. Cheng, O. Christiansen, M. Heckert, O. Heun, C. Huber, T. C. Jagau, D. Jonsson, J. Juslius, K. Klein, W. J. Lauderdale, D. A. Matthews, T. Metzroth, L. A. Mck, D. P. O’Neill, D. R. Price, E. Prochnow, C. Puzzarini, K. Ruud, F. Schiffmann, W. Schwalbach, C. Simmons, S. Stopkiewicz, A. Tajti, J. Vázquez, F. Wang, and J. D. Watts, “Cfour, coupled-cluster techniques for computational chemistry, a quantum-chemical program package,” See <http://www.cfour.de>.
- [34] H. Tao, T. K. Allison, T. W. Wright, A. M. Stooke, C. Khurmi, J. van Tilborg, Y. Liu, R. W. Falcone, A. Belkacem, and T. J. Martínez, *J. Chem. Phys.* **134**, 244306 (2011).
- [35] H. Tao, B. G. Levine, and T. J. Martínez, *J. Phys. Chem.*

A 113, 13656 (2009).